ORIGINAL ARTICLE

The hybrid force/position anti-disturbance control strategy for robot abrasive belt grinding of aviation blade base on fuzzy PID control

Hongyao Zhang [1,2,3] · Lun Li [1,2] · Jibin Zhao [1,2] · Jingchuan Zhao [1,2,3]

Abstract

The high-quality grinding of the aviation blade components with the industry robot presents tremendous challenges because of the complexity of blade surface. The hybrid force/position anti-disturbance control strategy is developed base on fuzzy PID control to improve the quality of grinding aviation blades. Firstly, according to gravity compensation technology, the perception of contact force is discussed to solve the contact force between the blades and abrasive belt machine. Then, the hybrid force/position anti-disturbance control strategy is designed to ensure the stability of robot automatic grinding system. The speed gain loop and the dual fuzzy PID control are introduced to enhance the anti-disturbance ability of the control system. Meanwhile, the analysis of stability and steady-state error for force control loop are performed to prove the validation of the feasibility of control system. Eventually, the simulation and experiments are carried out on the robot automatic grinding system. The experimental results reveal that the proposed control strategy can achieve better control effect and grinding quality compared with the traditional PID control.

Keywords Robotic grinding · Abrasive belt grinding · Hybrid force/position control · Dual fuzzy PID control · Aviation blade

1 Introduction

The aero blade is the core components of aero engines, the source of power for aero aircraft [1, 2]. The aero blade needs to bear the extremely adverse working conditions of high pressure, high temperature, high speed, and high alternating stress. The manufacturing dimensional accuracy and surface quality requirements of the blades are necessary conditions to ensure aerodynamic performance and safety performance [3, 4], even if tiny manufacturing defect will affect the dynamic characteristics and life cycle of the aircraft, and even cause engine fault and property loss [5]. Traditionally, blade

grinding mainly depends on the manual operation and special multi-axis NC grinding machine tool. Due to complexity of blade surface, it is difficult to ensure manufacturing accuracy and consistency of grinding quality for manual grinding [6], in which the skills and the experiences of operators determined the efficiency and quality. The special multi-axis NC grinding machine tool has poor flexibility and is undesirably expensive. As a new grinding style, robotic abrasive belt grinding receives wide concerns and widely developed for blade-manufacturing industry. The robotic abrasive belt grinding not only ensures the manufacturing accuracy and consistency of grinding quality, but also significantly reduces the costs [7, 8]. To remedy the deficiency of robotic accuracy, the contact force control is normally employed to improve the grinding accuracy. The non-uniform material removal for blades is achieved by analysis of the contact force control and material removal model [9]. The force control strategy is essential for the robotic grinding to achieve controllable material removal depth. To authors' knowledge, according to whether the force and position control are coupled, the robot contact force control can be divided into two categories: the former is the coupling control of force and position, which includes impedance control, sliding mode control, and so on, and the latter is the decoupling control of force and position, which includes the

✉ Hongyao Zhang
zhanghongyao@sia.cn

✉ Jibin Zhao
jbzhao@sia.cn

1 State Key Laboratory of Robotics, Shenyang Institute of Automation, Chinese Academy of Sciences, Shenyang 110016, China

2 Institutes for Robotics and Intelligent Manufacturing, Chinese Academy of Sciences, Shenyang 110169, China

3 University of Chinese Academy of Sciences, Beijing 100049, China

🕗 Springer

direct hybrid force/position control and indirect hybrid force/position control. Certainly, a multitude of intelligent control algorithms [10–12] have been proposed base on the two types of control strategy in recent years. Huang et al. [13] developed a robotic grinding system which primarily aims at adaptive trajectory planning and passive force control which cannot promote the accuracy of force control. Lopes et al. [14] researched a type of force-impedance control; the control algorithm can be applied for many tasks that involve robot end effector contact with environments of unknown stiffness. Hsieh et al. [15] argued that an optimal predicted fuzzy PI gain scheduling controller to achieve the constant turning force control. Lian et al. [16] claimed that model-free fuzzy controller controls the cutting force system in order to solve the obstacle of accurate mathematical model. However, the applicability of the proposed model-free fuzzy controller is difficult to ensure for the impedance control. The impedance control strategy generally requires an accurate mathematical model, which is suitable for some desktop-level robots to implement simple experiments. And the strategy is unable to control the position and force respectively, so it is not usually suited for the accurate control of the force and position, especially for industrial robot grinding operations. Sun et al. [17] proposed a novel control algorithm for robotic belt grinding turbine blade, which focuses on the position-based explicit control strategy to improve grinding performance. However, the hybrid force/position control is not elaborated in this research. Hu et al. [18] developed the force control subsystem to control the contact force independently, and the normal force control space is orthogonalized from the feed movement control space. Zhan et al. [19] claimed that the profile-adaptive compliant control algorithm is introduced into the hybrid movement-force control strategy to restrain their disturbance and reduce the errors of position and posture. Lee et al. [20] presented the adaptive position and force control strategy for n-DOF robot manipulator under unknown environment. The fuzzy neural networks are adopted to estimate the unknown model of robot manipulator, and the adaptive position and force control are developed by the proposed adaptive strategy. Kumar et al. [21] presented the hybrid force/position control strategy for the force and position control obstacle of constrained reconfigurable manipulators based on neural network. As aforementioned, the previous hybrid force/position control researches always need to switch force/position control mode frequently, which might decrease the stability of the control system. Moreover, the adaptability of these control strategies is not robust, and it is troublesome to apply for other control systems. These hybrid force/position control strategies also ignored the optimization of force control process, especially the field of anti-disturbance force control and accurate perception of contact force. Inspired by the indirect hybrid force/position control strategy, the hybrid force/position anti-disturbance control strategy for robot automatic grinding

aviation blade is proposed to apply to the robotic grinding system. The accurate perception of contact force is the prerequisite for robotic control system. Simultaneously, the characteristics of anti-disturbance are reflected by the speed gain loop and dual fuzzy PID control.

The outline of the article is organized as follows: Section 1 describes some background information about robot grinding control. In Section 2, the gravity compensation and perception of contact force will be carried out. The hybrid force/position anti-disturbance control strategy base on fuzzy PID control will be given in Section 3. In Section 4, the dual fuzzy PID control strategy will be proposed to improve the anti-disturbance of the control system; meanwhile, the analysis of stability and steady-state error is shown. The simulation and experimental analysis results will be presented in Section 5. Finally, the conclusions will be described in Section 6.

2 The perception of contact force for robot grinding process

The robot automatic grinding system presented by the research includes the industry robot, force sensor, and abrasive belt machine. The force sensor is used to sense the contact force, of which one side is fixed to the robot and the other side is connected to the blade. With the flexibility of the robot, the aviation blade is ground on the abrasive belt machine. The controllability of the contact force must be ensured for robotic grinding or assembly operations [22–25], so the force control strategy is a significant link for robotic automatic machining. Simultaneously, the accurate contact force perception is a prerequisite for force control strategy. Generally, the force sensor is installed between the end of the robot and the actuator to measure the contact force information, which includes the preload of actuator, the zero drift value of the sensor, the load gravity of the actuator, and the contact force. As long as the influence of the preload of actuator, the zero drift value of the sensor and the load gravity of the actuator are eliminated, and the calculation of robotic installing angle is solved, the contact force can be obtained. The preload of actuator, the zero drift value of the sensor, the load gravity of the actuator, and the robotic installing angle are regarded as multi-source parameters. The gravity compensation technology is principally to identify the multi-source parameters to obtain contact force. The preload of actuator can be classified into the zero drift value of the sensor, that is, the zero drift value $^S F_{zero}$ which includes zero drift value of the sensor and preload of actuator. The zero drift value $^S F_{zero}$ can be described as $^S F_{zero} = (^s f_{xzero}, ^s f_{yzero}, ^s f_{zzero}, ^s m_{xzero}, ^s m_{yzero}, ^s m_{zzero})$.

The zero drift value $^s f_{xzero}, ^s f_{yzero}, ^s f_{zzero}, ^s m_{xzero}, ^s m_{yzero}, ^s m_{zzero}$, robotic installing angle ϕ, φ, the gravity of actuator g, and the center of gravity (x, y, z) 12 parameters should be

identified during gravity compensation. The previous multi-source parameter gravity compensation technology [26] is employed to complete the gravity compensation in the research. During the process of robot automatic grinding blades, it is necessary to accurately sense the contact force between the workpiece and the abrasive belt machine. According to the contact force, the grinding trajectory is corrected to achieve force control strategy. The high precision perception of the contact force is prerequisite and guarantees grinding quality of blades.

As depicted in Fig. 1, $O_0X_0Y_0Z_0$ is the established world coordinate system, $O_0X_1Y_1Z_1$ is base coordinate system of robot, $O_SX_SY_SZ_S$ is force sensor coordinate system, and $O_TX_TY_TZ_T$ is the established abrasive belt coordinate system. The force sensor is mounted on the robotic end flange, and the actuator is installed on the other side of the force sensor. The contact force which is parallel to the Z axis of $O_TX_TY_TZ_T$ is primarily concerned in this research. Many previous researches took the force of robot base coordinate system as contact force. Although the robot base coordinate system is fixed, the force of robot base coordinate system cannot truly reflect the contact force during process of the grinding. Therefore, only the force in the abrasive belt coordinate system can exactly represent the contact force of the grinding process. The contact force perception is that the force detected by the force sensor is transferred to the abrasive belt coordinate system through coordinate transformation. Through coordinate transformation, the contact force ^TF_c which is detected by the force sensor is decomposed to the abrasive belt coordinate system to achieve contact force perception.

According to the gravity compensation technology, the contact force detected can be obtained as follows,

$$^SF_c = {}^SF - {}^SG - {}^SF_{zero} \tag{1}$$

$^SF_{zero} = ({}^sf_{xzero}, {}^sf_{yzero}, {}^sf_{zzero}, {}^sm_{xzero}, {}^sm_{yzero}, {}^sm_{zzero})$ is known according to the gravity compensation technology. The gravity of actuator is $^SG = ({}^sg_x, {}^sg_y, {}^sg_z, {}^sm_{gx}, {}^sm_{gy}, {}^sm_{gz})$ in force sensor coordinate system, and ^SG can be described as,

$$
\begin{pmatrix} {}^sg_x \\ {}^sg_y \\ {}^sg_z \\ {}^sm_{gx} \\ {}^sm_{gy} \\ {}^sm_{gz} \end{pmatrix} = \begin{pmatrix} R_{11} & R_{12} & R_{13} \\ R_{21} & R_{22} & R_{23} \\ R_{31} & R_{32} & R_{33} \\ 0 & -z & y \\ z & 0 & x \\ -y & x & 0 \end{pmatrix} \begin{pmatrix} -g\sin\varphi \\ g\sin\phi\cos\varphi \\ -g\cos\varphi \\ {}^sg_x \\ {}^sg_y \\ {}^sg_z \end{pmatrix} \tag{2}
$$

^SF_c is calculated by substituting Eq. (2) into Eq. (1). And the contact force ^TF_c can be calculated as,

$$^TF_c = R_1^T \begin{pmatrix} R_{11} & R_{12} & R_{13} \\ R_{21} & R_{22} & R_{23} \\ R_{31} & R_{32} & R_{33} \end{pmatrix} {}^SF_c \tag{3}$$

where R_1^T represents the coordinate transformation from the robot base coordinate system to the abrasive belt coordinate system. And R_1^T can be calculated by teaching the robotic external tool coordinate system.

The gravity compensation strategy is applied to eliminate the influence of multi-source parameters. Ideally, when the actuator is not in contact with the abrasive belt machine, the calculated contact force is zero. As illustrated in Fig. 2, when gravity compensation is intervened, the contact force will remain around 0 N even if the robotic pose changes. The average of contact force is around -0.1896 N, the variance of contact force is 0.1918, and the accuracy of gravity compensation completely meets the requirements.

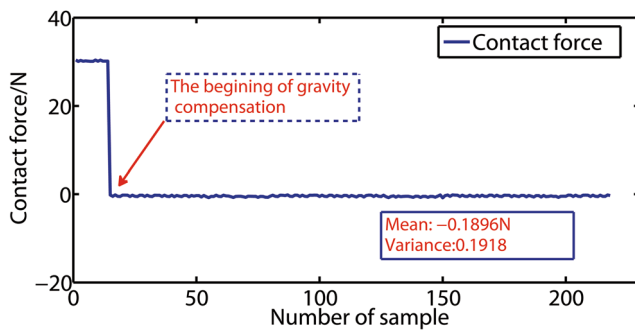Fig. 1 Relationship of all coordinate systems
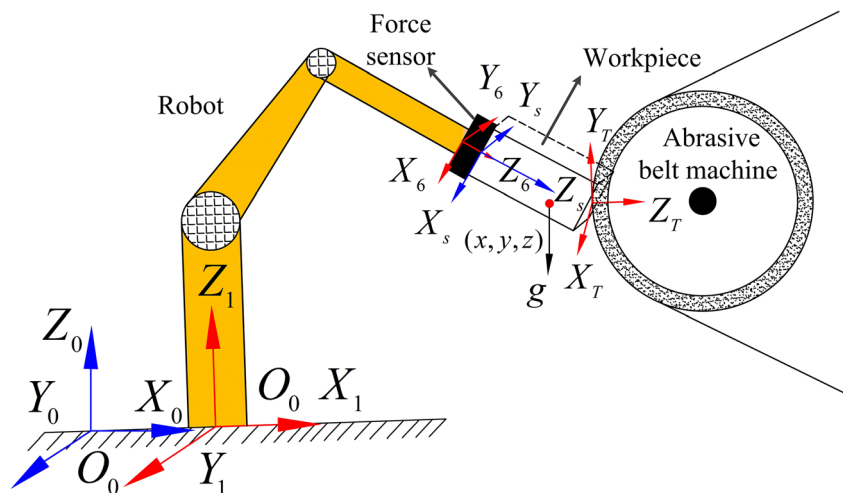
Fig. 2 Robot gravity compensation technology experiment results

3 The hybrid force/position anti-disturbance control strategy base on fuzzy PID control

During process of robot automatic grinding, the contact force changes drastically, and the control object is much complicated. Base on fuzzy PID control, this paper proposed the hybrid force/position anti-disturbance control strategy, which aims to promote the force compliance control during process of the grinding, and improve the quality and efficiency for the grinding blades. Simultaneously, the dual fuzzy PID control strategy is developed to improve the anti-disturbance of control system in the force control loop.

3.1 The brief introduction of fuzzy PID

PID control is a widely used and effective control method, which includes proportional, deviation, and integral control. The proportional control can reflect the signal deviation proportionally, the integral control can eliminate the static error of the control system, and the derivative control can improve the adjustment speed of the control system and adjust efficiency. The output of the PID controller can be calculated as,

$$u(k) = K_p e(k) + K_i T_c \sum_{i=0}^{k} e(i) + (K_d/T_c)\Delta e(k) \qquad (4)$$

where $e(k)$ is input deviation, T_c is time cycle, and $\Delta e(k)$ is deviation rate. K_p, K_i, K_d respectively represent the parameters of PID control. $u(k)$ is the output of PID control.

Although the PID control has a better control effect for linear systems, PID control cannot adapt to the nonlinear system with high complexity, especially uneven parameter changes and large system disturbances. The combination of fuzzy control and PID control, which is a kind of intelligent control, can make the control strategy more adaptable to the nonlinear system.

The essence of fuzzy PID control is to optimize the three parameters of the PID control system based on fuzzy control theory. According to the actual working conditions of the control object, three control parameters (ΔK_p, ΔK_i, ΔK_d)

are real-timely optimized to be more suitable for the control system.

As illustrated in Fig. 3, e and ec which are input of the fuzzy PID controller are, respectively, deviation and deviation rate of contact force. Firstly, K_p, K_i, K_d are obtained according to the traditional PID controller. Then, ΔK_p, ΔK_i, ΔK_d are calculated through the fuzzy controller. Finally, the PID parameters are given by,

$$\begin{aligned} K_p &= K_{p0} + \Delta K_p \\ K_i &= K_{i0} + \Delta K_i \\ K_d &= K_{d0} + \Delta K_d \end{aligned} \qquad (5)$$

The value of ΔK_p, ΔK_i, ΔK_d will be dynamically regulated according to the variation of e and ec. In contrast, the parameters of traditional PID control are invariable. Therefore, the fuzzy PID has a more excellent performance for nonlinear systems than traditional PID control.

3.2 The hybrid force/position anti-disturbance control strategy

As described in Fig. 4, the hybrid force/position anti-disturbance control strategy based on fuzzy PID control includes three loops: position control loop, force control loop, and speed gain loop. Among them, the hybrid force/position control composed of the force control loop and the position control loop. The speed gain loop can enhance the anti-disturbance ability of the control system by increasing the robot speed.

The switching of the hybrid force/position control depends on the selection matrix S, which is a 6 × 6 diagonal matrix (the robot has 6 degrees of freedom), and each element of the diagonal matrix represents a degree of freedom of the robot. When the value of element is 1, the degree of freedom is force control, and the element value is 0, the degree of freedom is position control. As described in Fig. 2, the force control strategy plays a role between the workpiece and the abrasive belt machine, which includes force/position control X_T, Y_T, Z_T and torque/posture A_T, B_T, C_T. During the process of robot automatic grinding, Z_T remains vertical with the contact surface which is between the workpiece and the abrasive belt machine. So the force control is performed in the Z_T direction, and position control is used for the X_T, Y_T, Z_T, A_T, B_T, C_T direction. As displayed in Fig. 5, the planned trajectory is applied to achieve position control. At the beginning of Z_T force control, the position control is achieved according to the planned trajectory, then the position value of Z_T direction is the sum of the robot current position value and the force correction value which is calculated by the deviation between the contact force and the reference force to achieve force
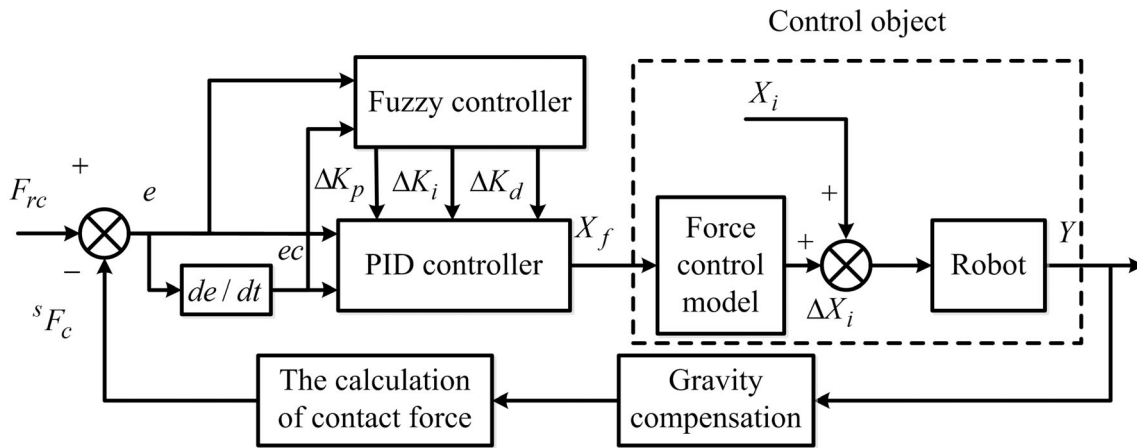
Fig. 3 Fuzzy PID control block diagram

control. So the selection matrix S can be expressed as $S = diag\,(0, 0, 1, 0, 0, 0)$.

According to the planned trajectory $x_p = (x_p, y_p, z_p, a_p, b_p, c_p)^T$ and robot current position value $x_r = (x_r, y_r, z_r, a_r, b_r, c_r)^T$, which is transmitted by the robot system, the position control loop can be described as,

$$x_n = S x_r + (I-S) x_p = \left(x_p, y_p, z_r, a_p, b_p, c_p\right)^T \quad (6)$$

According to robot inverse kinematics, the angle of the robotic joints can be calculated as,

$$\theta_n = \left(\alpha_{n1}, \alpha_{n2}, \alpha_{n3}, \alpha_{n4}, \alpha_{n5}, \alpha_{n6}\right)^T \quad (7)$$

For the force control loop, the contact force ${}^sF_c$ is analyzed according to the gravity compensation and the perception of contact force. F_{rc} is the reference force. So the deviation value

between the contact force and the reference force can be calculated by,

$$\Delta F_c = {}^sF_c - F_{rc} \quad (8)$$

The corresponding position control deviation Δx_{fn} is calculated according to the fuzzy PID force control strategy,

$$\Delta x_{fn} = \left(0, 0, z_{fn}, 0, 0, 0\right)^T \quad (9)$$

θ_{fn} can be obtained by robot inverse kinematics,

$$\theta_{fn} = \left(0, 0, \alpha_{fn}, 0, 0, 0\right)^T \quad (10)$$

The final joint angle of the robot can be calculated as,

$$\theta_e = \theta_n + \theta_{fn} = \left(\alpha_{n1}, \alpha_{n2}, \alpha_{n3} + \alpha_{fn}, \alpha_{n4}, \alpha_{n5}, \alpha_{n6}\right)^T \quad (11)$$
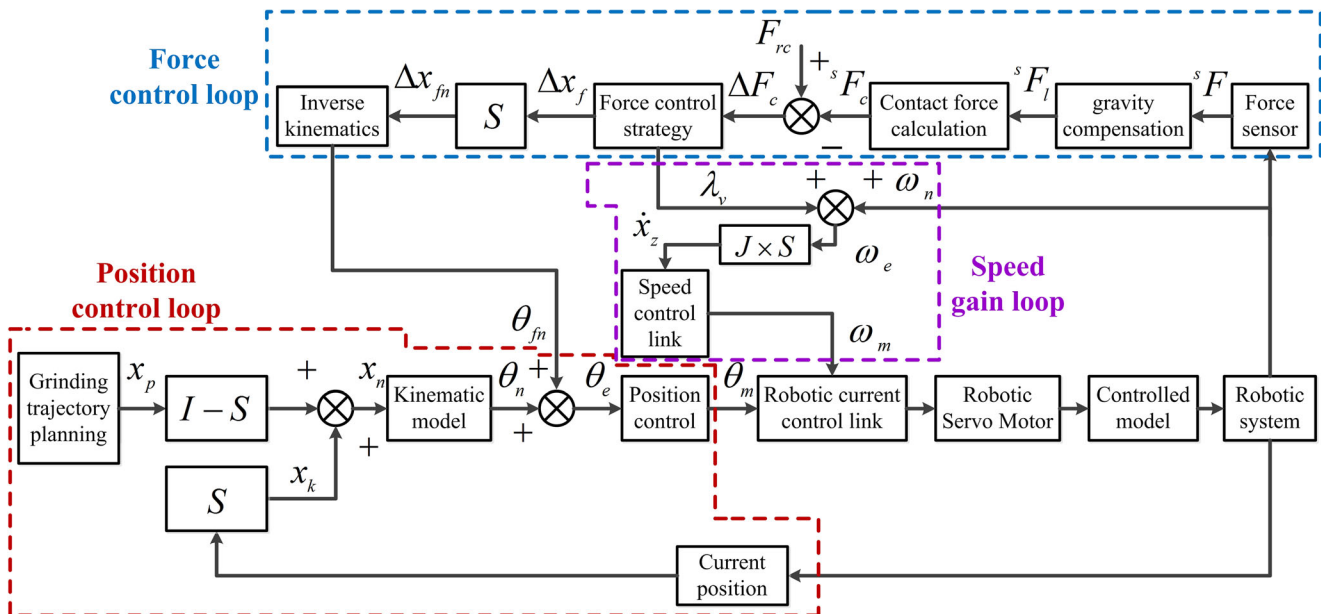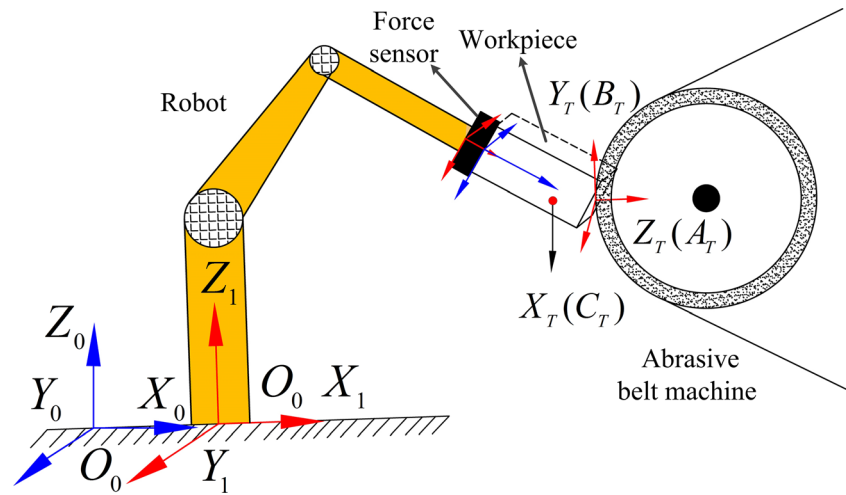

Fig. 4 Hybrid force/position anti-disturbance control strategy base on fuzzy PID control

Fig. 5 Contact force of robot automatic grinding

where θ_e is transferred to the robotic controller to achieve the hybrid force/position control.

Moreover, the speed gain loop is merged into the hybrid force/position control strategy to resist the sudden change and disturbance of contact force, because the robot automatic grinding is a nonlinear, irregular, and complicated process. Therefore, the speed gain loop can promote the anti-disturbance ability of the control strategy; that is, when the disturbance occurs, the robot speed increases to reduce the system response time.

λ_v is speed gain coefficient which is obtained by fuzzy PID controller according to the force deviation. The speed output $\dot{x}_z$ of the speed gain loop can be calculated by,

$$\omega_e = (\lambda_v\omega_{n1}, \lambda_v\omega_{n2}, \lambda_v\omega_{n3}, \lambda_v\omega_{n4}, \lambda_v\omega_{n5}, \lambda_v\omega_{n6}) \quad (12)$$

$$\dot{x}_z = \omega_e \times J \times S = (0, 0, v_z, 0, 0, 0)$$

When the force deviation ΔF_c is larger, the speed of direction Z_T will be increased, which aims to improve the response time and enhance the anti-disturbance ability of the control system.

4 The dual fuzzy control strategy

4.1 The dual fuzzy PID anti-disturbance control

In view of the above hybrid force/position control strategy, the dual fuzzy PID anti-disturbance control method is proposed for the force control loop. The control strategy can improve the accuracy of force control system, increases the response speed, and reduces overshoot. According to the fuzzy PID control strategy described in the previous section, the fuzzy subset of e, ec, ΔK_p, ΔK_i, ΔK_d is defined as {NB, NM, NS, ZO, PS, PM, PB}. According to the theoretical derivation and experimental results of this research, the range of contact force

which is usually used in the robot automatic grinding blade is 0 N–30 N, the range of e is $-6N \le e \le 6N$, and the range of ec is $-9 \le ec \le 9$. Meanwhile, when the range of K_p, K_i, K_d is $-0.3 \le K_p \le 0.5, 0 \le K_i \le 0.48, -0.15 \le K_d \le 0.25$, the control system will have better performance for traditional PID control. So $K_{p0} = 0.1$, $K_{i0} = 0.24$, $K_{d0} = 0.05$ is set, and the fuzzy domain of ΔK_p, ΔK_i, ΔK_d can be defined as,

$$\Delta K_p\{-0.4, -0.27, -0.13, 0, 0.13, 0.27, 0.4\}$$
$$\Delta K_i\{-0.24, -0.16, -0.08, 0, 0.08, 0.16, 0.24\}$$
$$\Delta K_d\{-0.3, -0.2, -0.1, 0, 0.1, 0.2, 0.3\}$$

The fuzzy base domain of e, ec can be determined as,

$$e\{-6, -4, -2, 0, 2, 4, 6\} \, ec\{-9, -6, -3, 0, 3, 6, 9\}$$

The triangle membership function of which structure is simple and easy to program writing is employed in the fuzzy controller. The basic principle of fuzzy rules is given as follows: Initially, when the output error $|e|$ is lager, the larger K_p should be chosen to reduce the system response time, the lager K_d should be set to prevent overshooting, and $K_i = 0$ is determined to avoid integral saturation. Secondly, when the value of $|e|$ is smaller, the smaller K_p and K_i are chosen to keep the control system stable and decreased steady-state error. When $|ec|$ is lager, smaller K_d should be chosen. When value of $|ec|$ is smaller, the medium K_d should be set to suppress advanced error. Eventually, when the value of $|e|$ is medium, the smaller K_p should be chosen to prevent overshooting. When $|ec|$ is smaller, the smaller K_i and medium K_d are determined to suppress advanced error. When $|ec|$ is lager, the smaller K_p and K_i should be chosen. According to the above basic principle, the fuzzy rule base of e, ec - ΔK_p, ΔK_i, ΔK_d is demonstrated in Table 1.

The fuzzy base domain of $e\{-6, -4, -2, 0, 2, 4, 6\}$, $ec\{-9, -6, -3, 0, 3, 6, 9\}$ can cover most of the contact force situations, whereas the larger ec and e still exist because of complexity of control system and blade profile. Meanwhile, the

Table 1 Fuzzy rule base of e, ec - ΔK_p, ΔK_i, ΔK_d

$\Delta K_p \Delta K_i \Delta K_d$		ec						
		NB	NM	NS	ZO	PS	PM	PB
e	NB	PB/NB/PB	PB/NB/PB	PB/NB/PM	PM/NS/PS	PB/NB/PM	PB/NB/PB	PB/NB/PB
	NM	PM/NB/PB	PM/NM/PM	PS/NS/PS	ZO/ZO/ZO	PS/NS/PS	PM/NM/PM	PM/NB/PB
	NS	PM/ZO/PM	PS/NS/PS	ZO/NM/ZO	NS/NB/ZO	NM/NM/ZO	PS/NS/PS	PM/ZO/PM
	ZO	ZO/ZO/NB	NS/PS/NM	NM/PM/NS	NB/PB/NS	NM/PM/NS	NS/PS/NM	ZO/ZO/NB
	PS	PM/ZO/PM	NS/NS/PS	ZO/NM/ZO	NS/NB/ZO	NM/NM/ZO	PS/NS/PS	PM/ZO/PM
	PM	PM/NB/PB	PM/NM/PM	PS/NS/PS	ZO/ZO/ZO	PS/NS/PS	PM/NM/PM	PM/NB/PB
	PB	PB/NB/PB	PB/NB/PB	PB/NB/PM	PM/NS/PS	PB/NB/PM	PB/NB/PB	PB/NB/PB

value of e, ec which is beyond the scope of fuzzy base domain is unlikely to appear frequently. Obviously, it is not feasible for grinding process to expand blindly the scope of fuzzy base domain. Therefore, the dual fuzzy PID anti-disturbance control strategy is proposed to strengthen adaptability of control system.

As depicted in Fig. 6, the fuzzy PID controller FC1 is established according to the above method. And the fuzzy PID controller FC2 which relies on the converter *Switch* to control whether the controller FC2 is connected is introduced to promote the adaptability of the force control system. The rule of **Switch** is described as,

$$\text{Switch}\begin{matrix}\text{if } |e| \geq \delta on \\ \text{if } |e| < \delta off\end{matrix} \tag{13}$$

where δ is threshold of contact force error. When $|e| \geq \delta$, the fuzzy controllers FC1 and FC2 are employed simultaneously. When $|e| < \delta$, the fuzzy controller FC1 is employed, and the fuzzy controller FC2 is closed. e, ec are the input of fuzzy controller FC2, and the proportional coefficient λ_p and differential coefficient λ_d are the output of fuzzy controller FC2. Notably, according to the proportional coefficient λ_p and differential coefficient, K_p and K_d of the fuzzy controller FC1 regulated λ_d to adapt the situation beyond the base domain of e, ec.

For the fuzzy controller FC2, the base domain of e, ec can be described as,

$$e\{-18, -12, -6, 0, 6, 12, 18\} ec\{-21, -15, -9, 0, 9, 15, 21\}$$

Equally, the base domain of λ_p and λ_d can be defined as,

$$\lambda_p\{2.2, 2.0, 1.8, 1.6, 1.4, 1.2, 1.0\} \lambda_d\{2.0, 1.8, 1.6, 1.5, 1.4, 1.2, 1.0\}$$

The fuzzy subset of e, ec, λ_p, λ_d is defined as {NB, NM, NS, ZO, PS, PM, PB}. Also, the fuzzy rule base of e, $ec - \lambda_p$, λ_d is demonstrated in Table 2.

When $|e| < \delta$, the status of converter **Switch** is off, so ΔK_p, ΔK_i, ΔK_d which is obtained by the fuzzy controller FC1 can
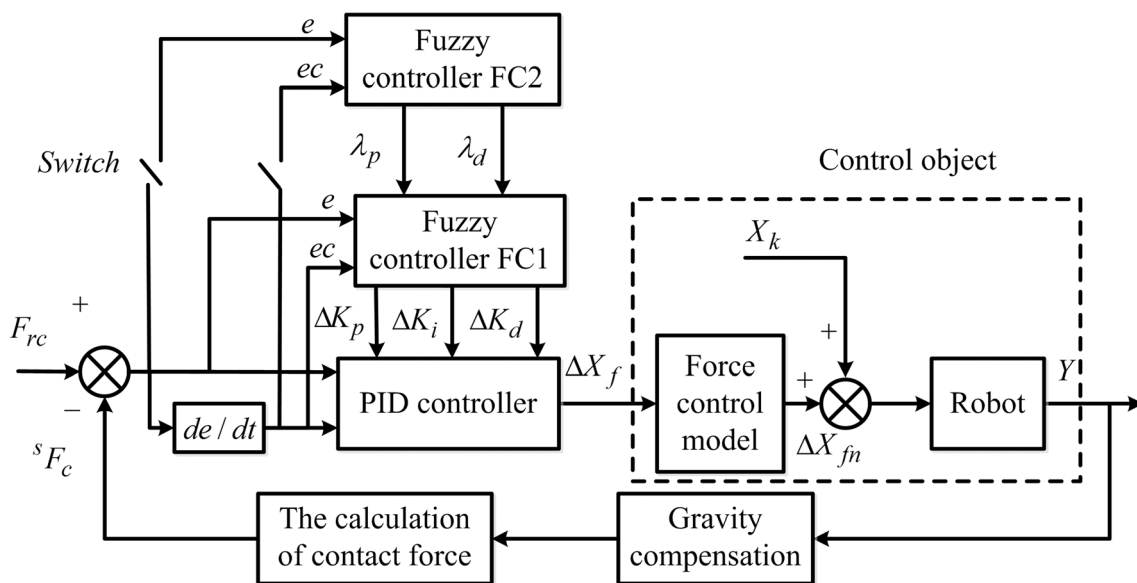
Fig. 6 Dual fuzzy PID anti-disturbance control strategy

Table 2 Fuzzy rule base of e, ec − λ_p, λ_d

λ_p, λ_d		ec						
		NB	NM	NS	ZO	PS	PM	PB
e	NB	PB /PB	PB/ PM	PB/PM	PB/PS	PB/PM	PB/PM	PB/PB
	NM	PB/PM	PM/PM	PM/PS	PS/PS	PM/PS	PM/PM	PB/PM
	NS	PM/ PS	PS/ZO	ZO/NS	NS/NB	ZO/NS	PS/ZO	PM/PS
	ZO	ZO/ZO	NS/NS	NM/NM	NB/NB	NM/NM	NS/NS	ZO/ZO
	PS	PM/PS	PS/ZO	ZO/NS	NS/NB	ZO/NS	PS/ZO	PM/PS
	PM	PB/PM	PM/PM	PM/PS	PS/PS	PM/PS	PM/PM	PB/PM
	PB	PB/PB	PB/PM	PB/PM	PB/PS	PB/PM	PB/PM	PB/NB/PB

be described as,

$$
\begin{aligned}
K_p &= K_{p0} + \Delta K_p \\
K_i &= K_{i0} + \Delta K_i \\
K_d &= K_{d0} + \Delta K_d
\end{aligned}
\tag{14}
$$

When $|e| \geq \delta$, the status of converter **Switch** is on; therefore, according to the fuzzy controller FC1 and the fuzzy controller FC1, ΔK_p, ΔK_i, ΔK_d can be described as,

$$
\begin{aligned}
K_p &= K_{p0} + \lambda_p \Delta K_p \\
K_i &= K_{i0} + \Delta K_i \\
K_d &= K_{d0} + \lambda_d \Delta K_d
\end{aligned}
\tag{15}
$$

4.2 The analysis of stability and steady-state error for force control loop

The force control loop is simplified to complete the analysis of stability and calculation of steady-state error. The force control loop is simplified as illustrated in Fig. 7.

F_{rc} is the reference force of force control system, ${}^sF_c$ is contact force which is measured by force sensor. K_{fc} is the fuzzy PID control loop, G_{rs} represents transfer function of robot control model, L_p represents the environmental stiffness between actuator and abrasive belt machine, and G_d is the transfer function of gravity compensation and perception of contact force loop. Therefore, G_{rs} can be represented by,

$$
G_{rs} = \frac{1}{T_r s + 1} \times \frac{1}{T_s s + 1}
\tag{16}
$$
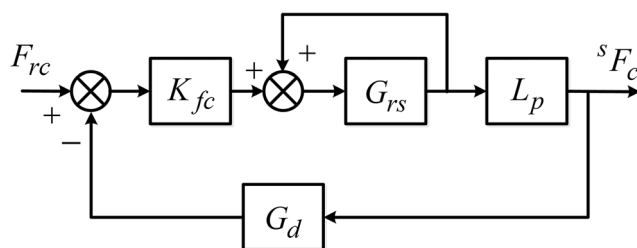
Fig. 7 Simplified force control loop

where T_r is the cycle period of control algorithm which is short enough to be ignored. T_s is the cycle period of robot system response which is 12 ms or 4 ms. Therefore, G_{rs} can be regarded as consecutive system. G_d can be described as,

$$
G_d = \frac{1}{T_d s + 1}
\tag{17}
$$

where T_d represents the cycle period of gravity compensation and perception of contact force. According to Fig. 7, the transfer function of the entire force control loop can be described as,

$$
\begin{aligned}
G(s) &= \frac{K_{fc} L G_{rs}}{K_{fc} L G_{rs} G_d + 1 - G_{rs}} \\
&= \frac{K_{fc} L_p (T_d s + 1)}{K_{fc} L_p + T_r T_s T_d s^3 + (T_r T_d + T_s T_d + T_r T_s) s^2 + (T_s + T_r) s}
\end{aligned}
\tag{18}
$$

According to characteristic equation of control system and Routh criterion, the stability condition of control system can be presented as,
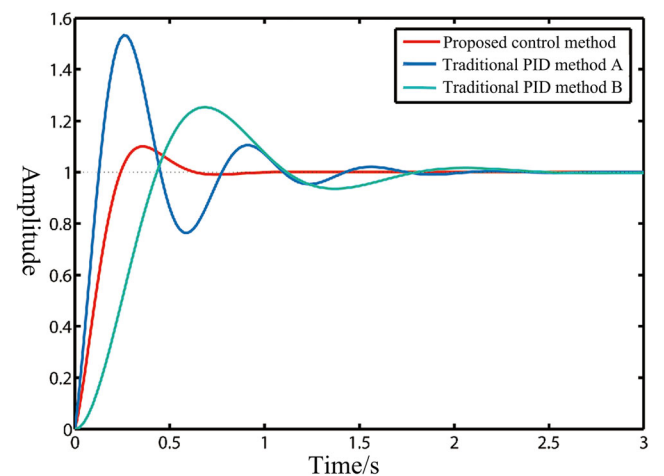
Fig. 8 Step response simulation comparison of three force control algorithms. The traditional PID control method A, K_p=0.35, K_i=0.2, K_d=0.1. The traditional PID control method B, K_p = 0.1, K_i = 0.2, K_d = 0.15

$$(T_r T_d + T_s T_d + T_r T_s)(T_s + T_r) - K_{fc} L_p T_r T_s T_d > 0 \quad (19)$$

The above Eq. (19) can be simplified as,

$$K_{fc} < \frac{(T_r T_d + T_s T_d + T_r T_s)(T_s + T_r)}{L_p T_r T_s T_d} \quad (20)$$

The stability condition of system can be evaluated as,

$$K_{fc} < \frac{2}{L_p} \quad (21)$$

The system error can be expressed as,

$$E(s) = F_{rc}(s) - {}^s F_c(s) G_d(s) = F_{rc}(s)(1 - G(s)G_d(s)) \quad (22)$$

The system steady-state error can be given in Eq. (22),

$$e_{ss} = \lim_{s \to 0} sE(s) = \lim_{s \to 0} sF_{rc}(s)(1 - G(s)G_d(s)) \quad (23)$$

When the system input is the pulse signal, that is $F_{rc}(s) = F_{rc}$, the steady-state error can be described as,

$$e_{ss} = \lim_{s \to 0} sE(s) = \lim_{s \to 0} sF_{rc}(1 - G(s)G_d(s)) = 0 \quad (24)$$

When the system input is the step signal, that is $F_{rc}(s) = F_{rc}/s$, the steady-state error can be described as,

$$e_{ss} = \lim_{s \to 0} sE(s) = \lim_{s \to 0} s\frac{F_{rc}}{s}(1 - G(s)G_d(s))$$
$$= \lim_{s \to 0} F_{rc}(1 - G(s)G_d(s)) = 0 \quad (25)$$

In summary, according to the Routh criterion, the force control system is stable.

5 Simulation and experimental analysis

The step respond simulation comparisons of the proposed control algorithms and two traditional PID control algorithms with different control parameters are illustrated in Fig. 8. Since the traditional PID control method A has a large proportional parameter, the system response is the rapid, but the cost is that the overshoot is as high as 50% or more, and the system oscillation is large. For the traditional PID control method B, although the overshoot is reduced and the oscillation is somewhat improved, the cost is that the response time increases. The proposed dual fuzzy PID anti-disturbance control strategy has fast response time, the small overshoot and the weakened oscillation.

The proposed control strategy is further validated by experiments on a 6-DOF KUKA KR 22 manipulator fitted with a six-axis ATI Min45Ti force sensor. As show in Fig. 9, the developed robot automatic grinding system also consists an
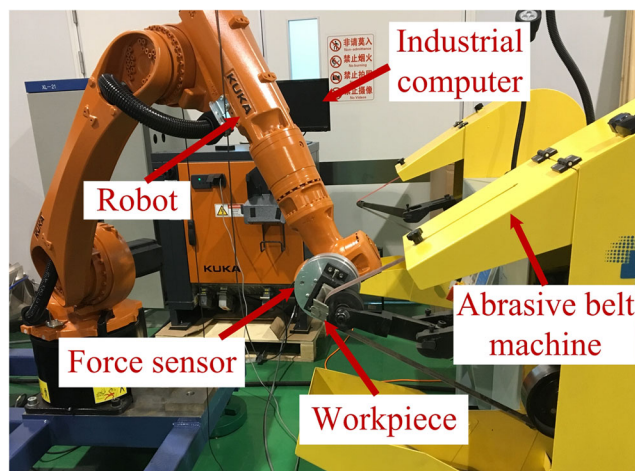

Fig. 9 Robot automatic grinding system

abrasive belt machine (SAMHIDA 2M5430GN), industrial computer (Advantech) running Microsoft Windows 7, a surface roughness tester (MAR), displacement sensor (Keyence GT2-PA12K), and binocular vision scanner which is developed by Shenyang institute of automation [27].

Furthermore, the grinding trajectory is planned according to CAD model of workpiece. The point cloud data which is obtained by the binocular vision scanner and displacement sensor is used for the calculation of machining allowance. In order to confirm the proposed force control algorithm, the 2 groups of different hybrid force/position control strategy experiments which include traditional PID force control and the dual fuzzy PID force control are carried out, and the experimental contact force is observed in Fig. 10. When the expected contact force is 15 N, the contact force with the proposed control strategy fluctuates in the range of 13 N~17 N compared with the range of 10 N~20 N in the circumstance of traditional PID control approach. The proposed control algorithm has better performance in terms of respond speed and force control accuracy compared with the traditional PID control method. The force control accuracy of the proposed hybrid force/position anti-disturbance control strategy is – 2 N~2 N (the force control accuracy 13.4%), while the accuracy of the traditional PID hybrid force/position control strategy is – 5 N~5 N (the force control accuracy 33.4%). Similarly, the response speed of the former is also faster than that of the latter, which can be recognized from the beginning point of force control. Furthermore, the control parameters K_p, K_i, K_d of the traditional PID control strategy are obtained by multiple experiments and trial-and-error method. Once the grinding parameters are changed, the control parameters K_p, K_i, K_d also need to change to improve the force control effect, which seriously affects the efficiency of grinding.

As illustrated in Fig. 11, the control parameter values of ΔK_p, ΔK_i, ΔK_d are monitored, which can change as the actual values of e and ec change to promote respond speed, control

Fig. 10 Comparison of dual fuzzy PID and traditional PID control experiments in the hybrid force/position control strategy
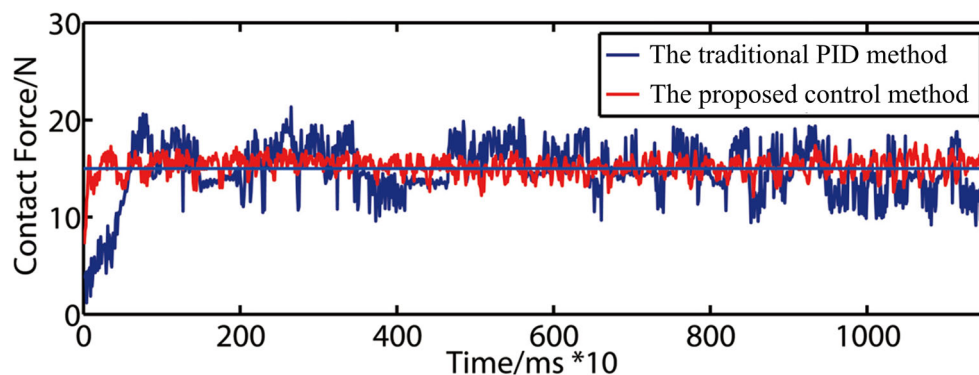
accuracy, and reduce the overshoot of the control system. For traditional PID control, the control parameters K_p, K_i, K_d always remain invariant during the control process, so the applicability of the proposed force control strategy is better than traditional PID control to improve the efficiency of grinding.

The anti-disturbance characteristic of dual fuzzy PID control is reflected at the few beginning points of grinding where the value of parameters ΔK_p and ΔK_d are larger, as shown in Fig. 10. Owing to the parameters e and ec is larger at the few beginning points, the fuzzy controller FC2 is activated for quick respond. The function of the dual fuzzy PID controller can not only improve the control effect at the few beginning points of the grinding but also cope with the force disturbance caused by the complexity of the blade profile and inaccurate positioning during the grinding process.

To further verify the favorable performance of the proposed control strategy, the results of two blades which are ground by the proposed control strategy and the traditional PID control are illustrated in Fig. 12. Furthermore, the control effect of contact force can also be reflected by the grinding surface quality which includes the material removal depth and surface roughness. The expected material removal depth is 0.0362 mm when the expected contact force is 15 N for developed robot grinding blade system. The blade which is

employed by the proposed strategy is shown in Fig. 12 a, and the blade which is employed by the traditional PID control is shown as b and c showing the comparisons of blade profile before and after grinding. The surface quality of the blade under the proposed strategy is more favorable than the blade under the traditional PID control. Additionally, the distribution of material removal depth and the surface roughness is illustrated in Fig. 13. Under the proposed control strategy, the mean of material removal depth is 0.0372 mm, the deviation from the desired material removal depth is 1.2 μm (the average error of 3%), the mean of surface roughness is 0.172 μm, and the standard deviation of surface roughness is 0.037. Under the traditional PID control strategy, the values respectively are 0.0446 mm, 7.7 μm (the average error of 21%), 0.622 μm, and 0.180. In conclusion, the developed robotic grinding system under the proposed control strategy can achieve more stable grinding contact force and better grinding quality.

6 Conclusion

In this paper, a control strategy is developed for robot automatic grinding system to achieve the high quality of grinding
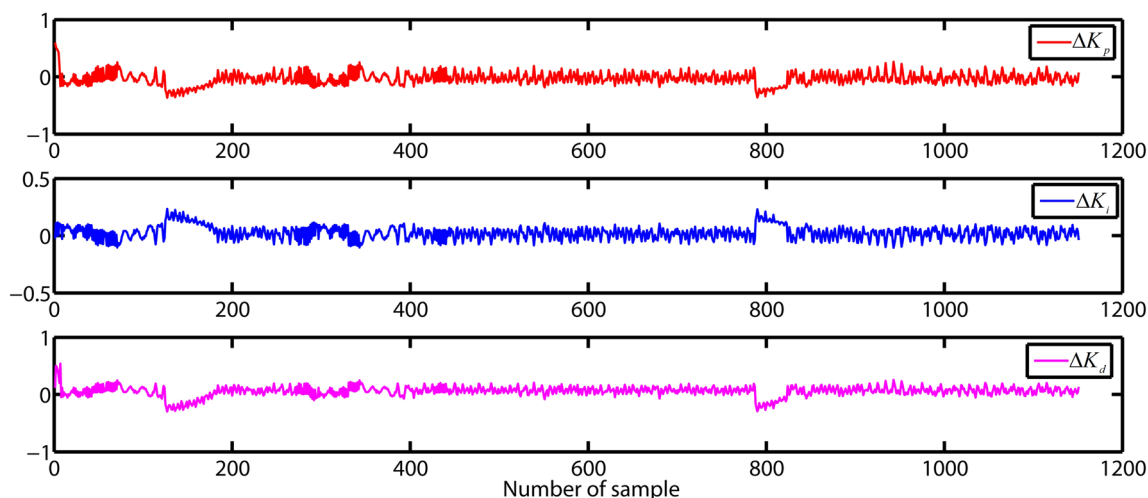
Fig. 11 Description of control parameters ΔK_p, ΔK_i, ΔK_d

Fig. 12 Experiment comparisons of surface quality and material removal depth. **a** The grinding results under the proposed control strategy. **b** The grinding results under the traditional PID control strategy. **c** The blade profile comparison between grinding after the proposed control strategy and before grinding
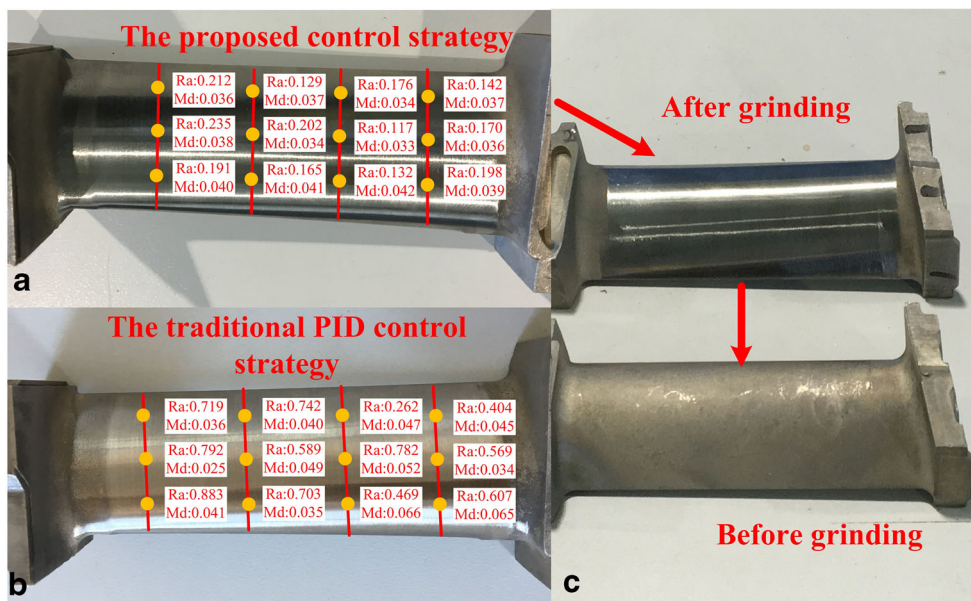
aviation blades. The main contributions of our research are drawn as follows:

(1) The perception of contact force approach was designed to evaluate the contact force between the blade and abrasive belt machine. A new control approach which is hybrid force/position anti-disturbance control strategy base on fuzzy PID control was addressed to achieve better control effect of the control system and grinding quality of the aviation blade.

(2) The speed gain loop was introduced into control system to enhance the ability anti-disturbance of the system. Meanwhile, the dual fuzzy PID control algorithm was also addressed for the first time to improve the anti-disturbance ability of the control system.

(3) Meanwhile, the robot automatic grinding system was established to achieve the blade grinding, and the simulation and experimental results show that the proposed control strategy has reliable advantages in stability of control system and surface quality of blades by comparing with the traditional PID. Compared with the traditional PID control, the control accuracy of contact force is improved from ±5 to ±2 N, the accuracy of material removal depth is improved from 7.7 to 1.2 μm, and the surface roughness of blades is improved from 0.622 to 0.172 μm.

The proposed research shows that the hybrid force/position anti-disturbance control strategy base on fuzzy PID control has great potential to achieve excellent surface quality and high grinding efficiency on the aviation blades. In addition, the proposed methodology is general and can be applied to robot automatic grinding other types of blades or workpieces.
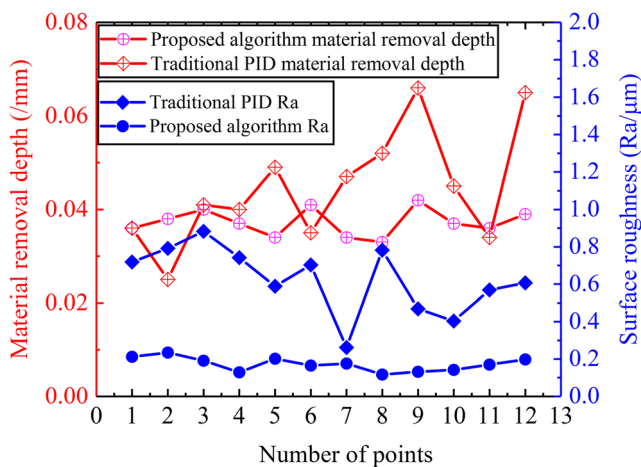
Fig. 13 Distribution of material removal depth and the surface roughness

Data availability The data used to support the findings of this paper is included within the article.

Declarations

Conflict of interest The authors declare no competing interests.

References

1. Wang H, Zhu D, Liu J (2019) Improving the accuracy of the blade leading/trailing edges by electrochemical machining with tangential feeding. Cirp Annals-manufact Technol 68(1):165–168
2. He W, Li Z, Guo Y, Cheng X, Zhong K, Shi Y (2018) A robust and accurate automated registration method for turbine blade precision metrology. Int J Adv Manuf Technol 97(9):3711–3721
3. Huang Z, Song R, Wan C, Wei P, Wang H (2019) Trajectory planning of abrasive belt grinding for aero-engine blade profile. Int J Adv Manuf Technol 102(1):605–614
4. Xu X, Zhu D, Zhang H, Yan S, Ding H (2017) TCP-based calibration in robot-assisted belt grinding of aero-engine blades using scanner measurements. Int J Adv Manuf Technol 90(90):635–647
5. Xu Z, Xu Q, Zhu D, Gong T (2013) A high efficiency electrochemical machining method of blisk channels. Cirp Annals-manufact Technol 62(1):187–190
6. Nagata F, Kusumoto Y, Fujimoto Y, Watanabe K (2007) Robotic sanding system for new designed furniture with free-formed surface. Robot Comput Integr Manuf 23(4):371–379
7. Hou B, Wang Y, Wang F, Ji Z, Liu H (2015) Research on belt grinding for marine propeller blade based on the second-order osculation. Int J Adv Manuf Technol 80(9):1855–1862
8. Zhao T, Shi Y, Lin X, Duan J, Sun P, Zhang J (2014) Surface roughness prediction and parameters optimization in grinding and polishing process for IBR of aero-engine. Int J Adv Manuf Technol 74(5):653–663
9. Wang W, Liu F, Liu Z, Yun C (2017) Prediction of depth of cut for robotic belt grinding. Int J Adv Manuf Technol 91(1):699–708
10. Yan S, Xu X, Yang Z, Zhu D, Ding H (2019) An improved robotic abrasive belt grinding force model considering the effects of cut-in and cut-off. J Manuf Process:496–508
11. Kiguchi K, Fukuda T (2000) Position/force control of robot manipulators for geometrically unknown objects using fuzzy neural networks. IEEE Trans Ind Electron 47(3):641–649
12. Nagata F, Mizobuchi T, Tani S, Watanabe K, Hase T, Haga Z, & Habib MK (2009). Impedance model force control using neural networks for a desktop NC machine tool. international symposium on industrial electronics.
13. Huang H, Gong ZM, Chen X, Zhou L (2002) Robotic grinding and polishing for turbine-vane overhaul. J Mater Process Technol 127(2):140–145
14. Lopes AM, De Almeida FA (2008) A force-impedance controlled industrial robot using an active robotic auxiliary device. Robot Comput Integr Manuf 24(3):299–309
15. Hsieh C, Chou J, Wu Y (2002) Optimal predicted fuzzy PI gain scheduling controller of constant turning force systems with fixed metal removal rate. Int J Adv Manuf Technol 19(10):714–721
16. Lian R, Lin B, Huang J (2006) Self-organizing fuzzy control of constant cutting force in turning. Int J Adv Manuf Technol 29(5):436–445
17. Du H, Sun Y, Feng D, Xu J (2015) Automatic robotic polishing on titanium alloy parts with compliant force/position control. Proc Inst Mech Eng B J Eng Manuf 229(7):1180–1192
18. Hu L, Zhan J (2014) Study on the orthomogonalization for hybrid motion/force control and its application in aspheric surface polishing. Int J Adv Manuf Technol 77:1259–1268. https://doi.org/10.1007/s00170014-6499-7
19. Zhan J, Yu S (2011) Study on error compensation of machining force in aspheric surfaces polishing by profile-adaptive hybrid movement force control. Int J Adv Manuf Technol 54(9):879–885
20. Lee C, Wang W (2016) Robust adaptive position and force controller design of robot manipulator using fuzzy neural networks. Nonlinear Dyn 85(1):343–354
21. Kumar N, Rani M (2020) Neural network-based hybrid force/position control of constrained reconfigurable manipulators. Neurocomputing.
22. Zhsao P, Shi Y (2013) Composite adaptive control of belt polishing force for aero-engine blade. Chin J Mechan Eng 26(5):988–996
23. Li Y, Zhang Z, Ye X, Chen S (2016) A novel micro-assembly method based on the mapping between assembly force and position. Int J Adv Manuf Technol 86:227–236
24. Jasim IF, Plapper PW (2014) Contact-state monitoring of force-guided robotic assembly tasks using expectation maximization-based Gaussian mixtures models. Int J Adv Manuf Technol 73(5):623–633
25. Tian F, Li Z, Lv C, Liu G (2016) Polishing pressure investigations of robot automatic polishing on curved surfaces. Int J Adv Manuf Technol 87(1-4):639–646
26. Zhang H, Li L, Zhao J, Zhao J, Liu S, Wu J (2020) Design and implementation of hybrid force/position control for robot automation grinding aviation blade based on fuzzy PID. Int J Adv Manuf Technol:1–14
27. Chen S, Xia R, Zhao J, Zhang H, Hu M (2017) Analysis and reduction of phase errors caused by nonuniform surface reflectivity in a phase-shifting measurement system. Opt Eng 56(3):033102